

1 Effects of particle breakage on the compression behaviour of gap
2 graded carbonate sand–silt mixtures

3 **Authors:** L. Ma, C.F. Chiu*, Y.P. Cheng, Y.Z. Ren

4

5 **Information of the authors**

6 **First author:** L. Ma

7 Ph.D. student, Key Laboratory of Ministry of Education for Geomechanics and Embankment
8 Engineering, Hohai University, Nanjing, China.

9 E-mail: malu1988@126.com

10 ***Corresponding author:** Abraham C.F. Chiu

11 Professor, Guangdong Engineering Center for Structure Safety and Health Monitoring, Shantou
12 University, Shantou, China.

13 E-mail: acf_chiu@stu.edu.cn

14 **Co-author:** Y.P. Cheng

15 Associate professor, Department of Civil, Environmental and Geomatic Engineering, University
16 College London, UK.

17 E-mail: yi.cheng@ucl.ac.uk

18 **Co-author:** Y.Z. Ren

19 Postgraduate student, Key Laboratory of Ministry of Education for Geomechanics and Embankment
20 Engineering, Hohai University, Nanjing, China.

21 E-mail: 714632754@qq.com

22

23 **Word Count: 2900**

1 **Abstract**

2 Isotropic compression tests were conducted on a series of gap graded mixtures of a carbonate sand
3 (CS) from the South China Sea and a fine crushed quartz silt to reveal how particle breakage of the
4 CS can affect the compression behaviour of these soil mixtures. The weaker CS originally exhibited
5 a unique compression line whereas the stronger quartz silt originally had a stable soil fabric leading
6 to non-convergent compression lines. It was found that the threshold fines content (FC) indicating
7 a change from CS to silt dominated soil matrix, together with the suppression of particle breakage,
8 have governed the change from converging to non-converging compression behavior and from
9 non-stable to stable soil fabric for these gap graded soil mixtures. For $FC \leq 30\%$, the soil mixtures
10 exhibited a unique compression line because of the substantial breakage of the weaker CS particles
11 in the CS dominated soil matrix. However, for $FC \geq 40\%$ (threshold FC), non-convergent
12 compression lines were observed for the soil mixtures. It was suggested that since the weaker CS
13 particles did not actively participate in load bearing of the silt dominated soil matrix, there was
14 insignificant particle breakage of the CS and the initial soil fabric remained stable at high stress
15 level.

16

17 **Key words:** calcareous soils, silts, compressibility, particle crushing

18

19

20

21

22

23

24

25

1. Introduction

Understanding the mechanical behaviour of gas hydrate bearing sediments is crucial for modelling the geotechnical related gas exploitation problems in the potential gas hydrate reservoirs. Recent studies on the silt and silty clay sediments taken from the South China sea have shown that gas hydrate was found in the fine-grained sediments containing substantial amount of foraminifera (Wang et al. 2011, Liu et al. 2012). Foraminifera fossils are shells of carbonate, which can be larger than silty particles, containing abundant intra-particle voids. These features of carbonate fossils can enhance the formation of gas hydrate in the fine-grained sediments. Past studies have revealed that some fine-grained soils like clayey silts and silty clays can exhibit non-convergent compression lines where the compression behaviour depends significantly on initial density (Nocilla et al. 2006, Shipton & Coop 2012). This was referred to as transitional soil behaviour. On the other hand, a unique compression line can be identified for coarse-grained soils like carbonate sand (CS) as breakage of sand particles at high stress level can erase the effects of initial soil structures leading to the more stable soil fabric (Coop 1990, Leleu & Valdes 2007, Miao & Airey 2013). This is the typical critical state soil behaviour. However, the compression behaviour of gap graded mixtures of coarse and fine grained soils is more complicated. It is important to understand the behaviour of these gap graded mixtures before further investigating the hydrate-bearing soils in the South China Sea.

Previous studies on sand-fines mixtures mostly focused on quartz sands (Ni et al. 2004, Yang et al. 2006b, Chiu & Fu 2008, Rahman et al. 2008). A threshold fines content (FC) can be observed to distinguish a sand or fines dominant soil matrix (Thevanayagam 1998, Thevanayagam et al. 2002). In sand-fines mixtures where the FC is above the threshold value, fines are the major components and play a dominant role in soil skeleton. As a result, sand grains take an insignificant part in the strong force chains of soil mixture (Minh & Cheng 2013, Minh et al. 2014), and vice versa. Grain mineralogy is one of the factors governing the type of compression behaviour of soil mixtures (Ponzoni et al. 2017, Nocilla et al. 2019). Recent studies on binary mixtures of different mineralogies have shown that a unique compression line was identified for the mixtures containing larger grains of a weaker type (e.g. carbonate) regardless of the proportion (Ponzoni et al. 2017). This paper presents how the FC of a fine-grained soil that initially exhibits stable soil fabric affects

1 the compression behaviour of CS–fines mixtures, and the laboratory test results are discussed based
2 on the concepts of particle breakage and threshold FC.

3

4 2. Materials and methodology

5 The tested soils were a CS and a non–plastic fine–grained crushed quartz silt. The two soils were
6 commercial products with different mineralogies. The CS was taken from a shallow water seabed
7 of the South China Sea consisting of angular and shelly carbonate particles of low sphericity. The
8 crushed quartz silt was taken from a quarry. The specific gravity of the CS and silt are 2.77 and 2.63,
9 respectively. Five different CS–silt mixtures were formed by mixing 20, 30, 40, 60 and 80% by dry
10 weight of silt (fines) to the CS. The particle size distribution (psd) of the soil mixtures, shown as the
11 solid lines in Fig. 1, were determined by the sieve and hydrometer analysis. The CS is a uniform
12 sand with average particle size (D_{50}) of 0.75 mm, and the silt size are between 5 and 75 μm and its
13 d_{50} is 43 μm . Thus, the size ratio R (D_{50} / d_{50}) is about 17.4. It is observed that the soil mixtures with
14 FC between 20 and 80% are gap–graded soils. The maximum and minimum void ratios of the soil
15 mixtures are presented in Fig. 2 as the solid lines. They initially decrease with increasing FC until
16 reaching a threshold value at 40% FC, after which the void ratios increase. The trough and this
17 threshold FC denote the transition between coarse and fine grained dominated soils (Lade et al.
18 1998, Zuo & Baudet 2015). For FC below 40%, CS plays a dominant role in the soil mixture and
19 vice versa. The observed threshold FC of the tested soils is higher than those reported in the literature.
20 Based on the sand–fines mixture with a size ratio R between 10 and 15, several studies (Yang et al.
21 2006a, Papadopoulou & Tika 2008, Dash et al. 2010) have revealed a threshold FC between 20 and
22 30%.

23 Isotropic compression tests were conducted on specimens 50 mm in diameter and 100 mm in
24 height using a high pressure triaxial apparatus. A total of 19 isotropic compression tests were
25 conducted. Specimens of each specific mixture ratio were compacted to reach two or three different
26 initial relative densities (between 20 and 90%) using the moist tamping method (MT) with an
27 undercompaction procedure to minimise the amount of segregation as well as to create uniform
28 specimens with a wide range of void ratio (Ladd 1978, Ishihara 1993, Fourie and Papageorgiou
29 2001, Yang and Liu 2016). Each specimen was compacted inside a split mould in 5 layers at an

1 initial water content of 5% using a special design compaction tool similar to the one presented in
2 [Ng and Chiu \(2003\)](#). For a D_r of 20%, it was found that the bottom layer was undercompacted to a
3 density 10% lower than the target density and the density increases linearly from the bottom to the
4 top layer. However, no specific tests were conducted to examine uniformity and segregation of
5 specimen. Further work, such as epoxy impregnation ([Yamamuro et al. 2008](#)) and X-ray tomography
6 ([Thomson and Wong 2008](#)) could be carried out to evaluate these two issues for MT specimen.

7 Saturation of specimen was conducted in two stages. Specimen was first flushed by de-aired
8 water slowly from its bottom under a vacuum of 15 kPa. Thereafter a back pressure of 800 kPa was
9 applied to saturate the specimen. The pore pressure parameter B of all specimens has reached a
10 minimum value of 0.95. The specimens were then isotropically compressed using a multiple-step
11 loading until reaching a maximum effective stress of 30 MPa. It should be noted that the volumes
12 of two solid constituents (CS and silt) were calculated separately based on the corresponding weight
13 and specific gravity to determine the void ratio of the soil mixtures. The initial void ratio was
14 evaluated from the initial dry weight and average dimensions of specimen. After the compression
15 test, the final void ratio of specimen was determined by the gravimetric method based on its final
16 water content. Freezing of the specimen and its membrane was performed to minimise the loss of
17 water during disassembling ([Sladen and Handford 1987](#)). By comparing the initial void ratio, change
18 in void ratio during compression and the final void ratio, it is found that the collapse of specimen
19 during saturation is insignificant.

20

21 3. Compressibility

22 [Figs. 3\(a\) to 3\(c\)](#) depict the isotropic compression curves for five different CS–silt mixtures
23 compacted at different initial dry densities. The compression curves for 0% FC (100% CS) and
24 100% FC are also shown in the figure for comparison. It is apparent that the compression curves
25 can be classified into two different trends. [Fig. 3 \(a\)](#) shows the compression curves of CS–silt
26 mixtures with $FC \leq 30\%$. The compression curves of each of these soil mixtures converge to a
27 unique line at a high effective stress of 30 MPa. The estimated normal compression line (NCL) for
28 each soil mixture is shown as a dotted line. The gradient of NCL decreases with increasing FC. The
29 0% FC exhibits a unique compression line as expected. It is evident that the type of compression

1 behaviour remains identical by adding to as much as 30% FC. This infers that, within this range, CS
2 particles remains the dominant component and silt particles do not significantly participate in the
3 load bearing mechanism. Breakage of the CS particles is significant in these soil mixtures leading
4 to a unique compression line in the high stress regime. Evidence of particle breakage will be
5 discussed in the next section. Figs. 3(b) and 3(c) show the compression curves of the CS–silt
6 mixtures with $FC \geq 40\%$ (threshold value). For the range of stress tested, the 100% FC (crushed
7 quartz silt) exhibits non–unique compression lines due to an initial stable soil fabric. It is apparent
8 that the same type of compression behaviour is observed for the soil mixtures with $FC \geq 40\%$. For
9 $FC \geq$ threshold value, the fine–grained silt is the dominant component in the soil mixtures such
10 that the CS particles have a reduced role in the load bearing mechanism. Hence, initial soil fabrics
11 are difficult to be altered by the displacement of particles leading to different compression curves.

12 Figs. 4(a) to 4(c) show the compression index evaluated at different effective stress. For each
13 stress increment, compression index is defined as the ratio between change in void ratio and change
14 in logarithm of effective stress. Two different trends are observed. For the majority of compression
15 curves (15 out of 19), the compression index increases with increasing stress until reaching a peak
16 or plateau. Thereafter, the compressibility reduces with further loading. Compared to the soil
17 mixtures with $FC \geq 40\%$, the trend of compression index for soil mixtures with $FC \leq 30\%$ reaches
18 the peak value at a lower stress (between 10 and 20 MPa) and exhibits a higher post-peak reduction
19 in compressibility (between 30 and 65% of the peak value). For the remaining four compression
20 curves (42 and 62% D_r for 60% FC, 40 and 61% D_r for 80% FC), the compressibility increases with
21 increasing stress. It is also apparent that the rate of increase in compression index becomes mild at
22 the stress of 30 MPa, except the specimen 42% D_r for the soil mixture with 60% FC. It is probable
23 the compression curves of 60% FC would converge if a higher stress was applied. Thus, further
24 compression tests beyond 30 MPa should be conducted to verify the hypothesis that the compression
25 curves of 60% FC do not converge to a unique line.

26

27 4. Particle Breakage

28 Past studies have shown that particle breakage is an important mechanism governing the
29 compression behaviour (Leleu & Valdes 2007, Miao & Airey 2013, Guida et al. 2018). Fig. 1 shows

1 the psd curves before and after compression tests. Before compression tests, there is negligible
2 amount of particles smaller than $5 \mu\text{m}$ for the tested soils. For the psd curves measured after
3 compression test, only specimens compacted to the lowest D_r for each soil mixture are presented in
4 the figure for clarity. It is apparent that negligible particle breakage is found for mixtures with a FC
5 $\geq 60\%$. On the other hand, there is a significant amount of particle breakage and the particle sizes
6 can reach as small as $2 \mu\text{m}$ for mixtures with a FC $\leq 30\%$. A parameter relative breakage, B_r (Hardin
7 1985) was adopted to quantify the amount of breakage. B_r is defined as the ratio of total breakage
8 to breakage potential. Breakage potential is the area enclosed by particle size $d = 75 \mu\text{m}$ and the
9 initial psd curve. Total breakage is the area enclosed by the initial and final psd curves. For B_r equals
10 to 0, there is no particle breakage. For B_r equals to 1, the particle sizes are smaller than $75 \mu\text{m}$ after
11 breakage. McDowell & Bolton (1998) revealed that particle breakage can lead to an ultimate psd
12 curve such that B_r cannot reach a value of 1. If the ultimate psd curve is available, a modified
13 breakage parameter proposed by Einav (2007) will be an alternative parameter to quantify particle
14 breakage. As a first approximation B_r was adopted in this study to estimate the extent of particle
15 breakage after compression test.

16 B_r is plotted against FC and shown in Fig. 2. For each soil mixture, B_r is evaluated for the
17 highest and lowest D_r specimens. It is found that B_r is negligible for FC $\geq 40\%$, but it increases
18 substantially to above 15% for FC $\leq 30\%$. For FC smaller than the threshold FC (40%), coarse-
19 grained CS is the dominant component in the soil matrix. Particle breakage is substantial that can
20 erase the effects of initial soil fabric. Thus, the compression curves of different initial densities
21 converge to a unique compression line. However, negligible amount of particle breakage is observed
22 above the threshold FC. Hence, the initial soil fabric still affects the compression behaviour and the
23 compression curves do not converge at high stress. Fig. 2 also indicates that the lowest D_r specimens
24 exhibit more particle breakage than the highest D_r specimens for FC $\leq 30\%$. The effect of density
25 on particle breakage is similar to the trend reported in Altuhafi and Coop (2011) for carbonate sand
26 mainly composed of broken shell fragments. McDowell and Bolton (1998) suggested that
27 coordination number decreases with decreasing density resulting in a higher probability of particle
28 breakage. It should be noted that particle breakage may also occur during specimen preparation by
29 moist tamping method as weaker CS is more susceptible to crushing, but breakage should be more
30 pronounced for dense specimen due to higher compaction energy. The pre-test particle breakage of

1 a dense specimen affects the pre-yield part and yield stress of the compression curve. However
2 majority of particle breakage occurs after yielding of compression as suggested by Guida et al.
3 (2018). Further work should be conducted to further investigate the evolution of particle breakage
4 due to specimen preparation and at different stress level of compression.

5 The observed compression behaviour is different from that of the gap graded soil mixtures
6 reported in Ponzoni et al. (2017). Ponzoni et al. tested gap graded mixtures of carbonate (crushed
7 limestone) and quartz sands featuring a low size ratio R of 3 between the coarse carbonate sand and
8 the fine quartz sand. Unique compression lines were also observed from mixtures with 0, 20, 50, 80
9 and 100% FC content. The size ratio ($R = 17.4$) of the tested soils in this study is higher. Shire et al.
10 (2016) suggested that for a binary mixture there is a limiting size ratio (R_L), below which a fine
11 particle cannot fit between coarse particles such that the mixture cannot be considered as gap graded.
12 Based on a two-dimensional consideration of inter-void constrictions, Choo and Burns (2015) took
13 R_L as 2.4 for gap graded soils. Using a three-dimensional discrete element analysis, Shire et al.
14 (2016) showed that for $2 < R < 6$, an intermediate type of gap graded behaviour could occur when
15 fines play a reduced but significant role in stress transfer. As R increases further, the fines pack more
16 efficiently between coarse particles resulting in less contribution in stress transfer. Compared to the
17 fine quartz sand used in Ponzoni et al. (2007), the silt tested in this study plays a less active role in
18 the load bearing for FC below the threshold value, leading to a higher particle breakage of CS (see
19 Fig. 2). Furthermore the CS tested in this study contains intra-particle voids (shelly fragments).
20 Guida et al. (2018) studied the breaking mechanism of a highly porous granular material during
21 compression. It is found that the trend observed in the compression curve can be linked to the
22 evolution of number of surviving particles (no breakage) observed from X-ray tomography. And,
23 the particles with higher internal porosity are more likely to break. Thus, distribution of internal
24 porosity of CS particles is also a factor governing the trend of compression.

25

26 5. Conclusions

27 A series of isotropic compression curves for gap graded mixtures of coarse-grained carbonate sand
28 (CS) and fine-grained crushed quartz silt with size ratio of 17.4 are presented. The weaker CS
29 exhibits an originally unique compression line, but the stronger quartz silt has a stable soil fabric

1 leading to originally non-convergent compression lines. Particle breakage correlates well with the
2 change in compression behaviour for this gap graded soil mixtures from the transitional to unique
3 compression behaviour and from a stable to non-stable soil fabric. This is also related to the
4 threshold fines content (FC) at 40% that distinguishes between the coarse-grained sand and the
5 fine-grained silt dominated soil matrix. For mixtures with FC above and equals to 40%, breakage
6 of the CS particles is insignificant during compression (as is reflected in the negligible value of
7 relative breakage B_r) because fine-grained silt is the dominant component in the soil matrix and CS
8 particles does not actively participate in the load bearing. Thus, the initial soil fabrics of different
9 initial densities are not erased completely leading to non-convergent compression lines. However,
10 for FC below and equals to 30%, CS is the dominant component in the soil matrix which actively
11 participates in the loading bearing. Thus, the weaker CS particles break substantially (as reflected
12 in a high B_r) resulting in a considerable erosion of the initial soil fabrics and a unique compression
13 line at high stress.

15 Acknowledgments

16 The authors would like to acknowledge the financial support of Key projects of natural science
17 research in colleges and universities of Anhui Province (KJ2018A0539, KJ2020A0080) and
18 Fundamental Research Funds for the Central Universities (2019B13714).

22 References

- 23 Altuhafi, F.N. & Coop, M.R. (2011). Changes to particle characteristics associated with the
24 compression of sands. *Géotechnique* 61(6), 459–471.
- 25 Chiu, C.F. & Fu, X.J. (2008). Interpreting undrained instability of mixed soils by equivalent
26 intergranular state parameter. *Géotechnique* 58(9), 751–755.
- 27 Choo, H. & Burns, S.E. (2015). Shear wave velocity of granular mixtures of silica particles as a
28 function of finer fraction, size ratios and void ratios. *Granular Matters* 17, 567–578.

- 1 Coop, M.R. (1990). The mechanics of uncemented carbonate sands. *Géotechnique* 40(4), 607–626.
- 2 Dash, H.K., Sitharam, T.G. & Baudet, B.A. (2010). Influence of non-plastic fines on the response
3 of a silty sand to cyclic loading. *Soils & Foundations* 50(5), 695–704.
- 4 Einav, I. (2007). Breakage mechanics-part 1: Theory. *Journal of the Mechanics and Physics of Solids*
5 55(6), 1274–1297.
- 6 Fourie, A.B. & Papageorgiou, G. (2001). Defining an appropriate steady state line for Merriespruit
7 gold tailings. *Canadian Geotechnical Journal* 38(4), 695–706.
- 8 Guida, G., Casini, F., Viggiani, G.M.B., Ando E. & Viggiani G. (2018) Breakage mechanisms of
9 highly porous particles in 1D compression revealed by X-ray tomography. *Géotechnique Letter*
10 8, 155–160.
- 11 Hardin, B. (1985). Crushing of Soil Particles. *Journal of Geotechnical Engineering*, 111(10), 1177–
12 1192.
- 13 Ishihara, K. (1993). Liquefaction and flow failure during earthquakes. *Géotechnique* 43(3), 351–
14 451.
- 15 Lade, P.V., Liggio Jr., C.D. & Yamamuro, J.A. (1998). Effects of nonplastic fines on minimum and
16 maximum void ratios of sand. *Geotechnical Testing Journal*, 2(4), 336–347.
- 17 Ladd, R.S. (1978). Preparing test specimens using undercompaction. *Geotechnical Testing Journal*
18 1(1), 16–23.
- 19 Leleu, S.L. & Valdes, J.R. (2007). Experimental study of the influence of mineral composition on
20 sand crushing. *Géotechnique* 57(3), 313–317.
- 21 Liu, C., Ye, Y., Meng, Q., He, X., Lu, H., Zhang, J., Liu, J. & Yang, S. (2012). The characteristics
22 of gas hydrates recovered from shenhu area in the south china sea. *Marine Geology* 307–310, 22–
23 27.
- 24 McDowell, G. & Bolton, M. (1998). On the micromechanics of crushable aggregates. *Géotechnique*
25 48(5), 667–679.
- 26 Miao, G. & Airey, D. (2013). Breakage and ultimate states for a carbonate sand. *Géotechnique*
27 63(14), 1221–1229.
- 28 Minh, N.H. & Cheng Y.P. (2013). DEM investigation of Particle size distribution effect to one-
29 dimensional compression. *Géotechnique* 63(1), 44–53.

- 1 Minh, N.H., Cheng, Y.P. & Thornton, C. (2014). Common strong force subnetwork and
2 compressibility of polydisperse assemblies. *Granular Matters* 16, 69–78.
- 3 Nocilla, A., Zimbardo, M. & Coop, M.R. (2019). Role of particle characteristics in the compression
4 behaviour of gap-graded sands. *Soils & Foundations* 59(3), 783–788.
- 5 Nocilla, A., Coop, M.R. & Colleselli, F. (2006). The mechanics of an Italian silt: an example of
6 ‘transitional’ behaviour. *Géotechnique* 56(4), 261–271.
- 7 Ni, Q., Tan, T.S., Dasari, G.R. & Hight, D.W. (2004). Contribution of fines to the compressive
8 strength of mixed soils. *Géotechnique* 54, 561–569.
- 9 Ng, C.W.W. & Chiu, A.C.F. (2003). Laboratory study of loose saturated and unsaturated
10 decomposed granitic soil. *Journal of Geotechnical and Geoenvironmental Engineering* 129(6),
11 550–559.
- 12 Papadopoulou, A. & Tika, T. (2008). The effect of fines on critical state and liquefaction resistance
13 characteristics of non-plastic silty sands. *Soils & Foundations* 48(5), 713–725.
- 14 Ponzoni, E., Nocilla, A. & Coop, M.R. (2017). The behaviour of a gap graded sand with mixed
15 mineralogy. *Soils & Foundations* 57, 1030–1044.
- 16 Rahman, M.M., Lo, S.R. & Gnanendran, C.T. (2008). On equivalent granular void ratio and steady
17 state behavior of loose sand with fines. *Canadian Geotechnical Journal* 45, 1439–1455.
- 18 Shipton, B.J.I. & Coop, M.R. (2012). On the compression behaviour of reconstituted soils. *Soils &*
19 *Foundations* 52(4), 668–681.
- 20 Shire, T., O’Sullivan, C. & Hanley, K.J. (2016). The influence of fines content and size-ratio on the
21 micro-scale properties of dense bimodal materials, *Granular Matters* 18(52), 1–10.
- 22 Sladen, J. & Handford, G. (1987). A potential systematic error in laboratory testing of very loose
23 sands. *Canadian Geotechnical Journal* 24(3), 462–466.
- 24 Thomson, P.R. & Wong, R.C.K. (2008). Specimen nonuniformities in water-pluviated and moist-
25 tamped sands under undrained triaxial compression and extension. *Canadian Geotechnical*
26 *Journal* 45, 939–956.
- 27 Thevanayagam, S. (1998). Effect of fines and confining stress on undrained shear strength of silty
28 sands. *Journal of Geotechnical and Geoenvironmental Engineering* 124, 479–491.
- 29 Thevanayagam, S., Shenthan, T., Mohan, S. & Liang, J. (2002). Undrained fragility of clean sands,
30 silty sands, and sandy silts. *Journal of Geotechnical and Geoenvironmental Engineering* 128,

1 849–859.

2 Wang, X., Hutchinson, D.R., Wu, S., Yang, S. & Guo, Y. (2011). Elevated gas hydrate saturation
3 within silt and silty clay sediments in the shenhu area, south china sea. *Journal of Geophysical*
4 *Research Solid Earth* 116, B5.

5 Yamamuro, J.A., Wood, F.M. & Lade, P.V. (2008). Effect of depositional method on the
6 microstructure of silty sand. *Canadian Geotechnical Journal* 45, 1538–1555.

7 Yang, S., Lacasse, S. & Sandven, R. (2006*a*). Determination of the transitional fines content of
8 mixtures of sand and non-plastic fines. *Geotechnical Testing Journal* 29(2), 102–107.

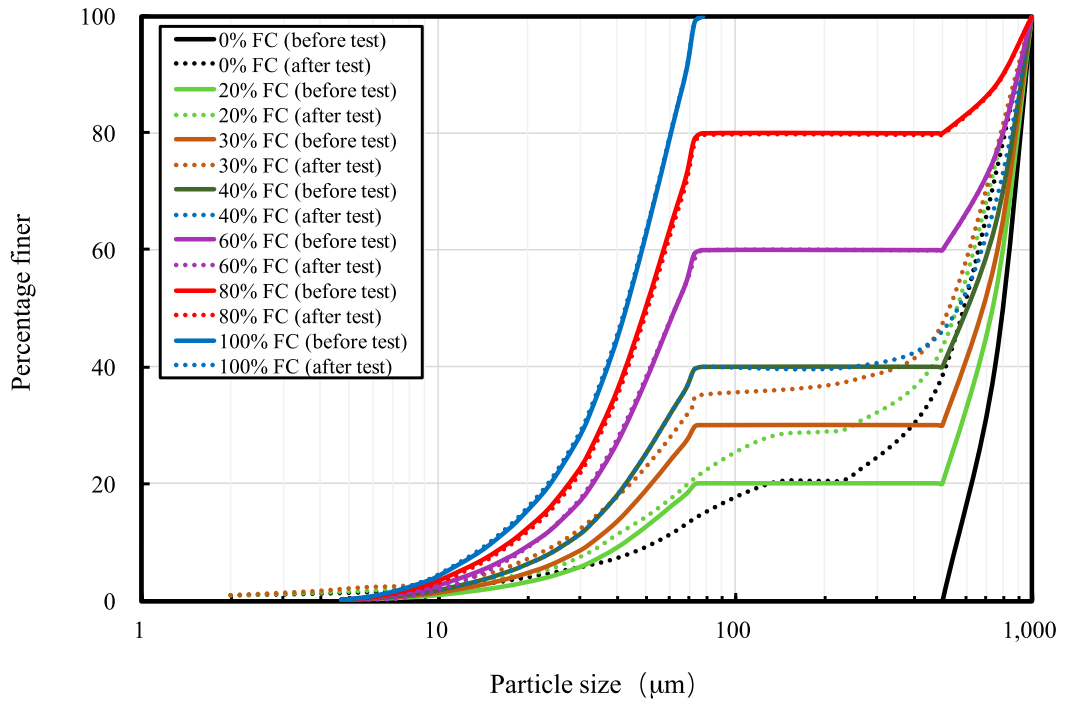
9 Yang, J. & Liu, X. (2016). Shear wave velocity and stiffness of sand: the role of non–plastic fines.
10 *Géotechnique* 66(6), 500–514.

11 Yang, S.L., Sandven, R. & Grande, L. (2006*b*). Instability of sand-silt mixtures. *Soil Dynamics and*
12 *Earthquake Engineering* 26, 183–190.

13 Zuo, L. & Baudet, B.A. (2015). Determination of the transitional fines content of sand-non plastic
14 fines mixtures. *Soils and Foundations* 55(1), 213–219.

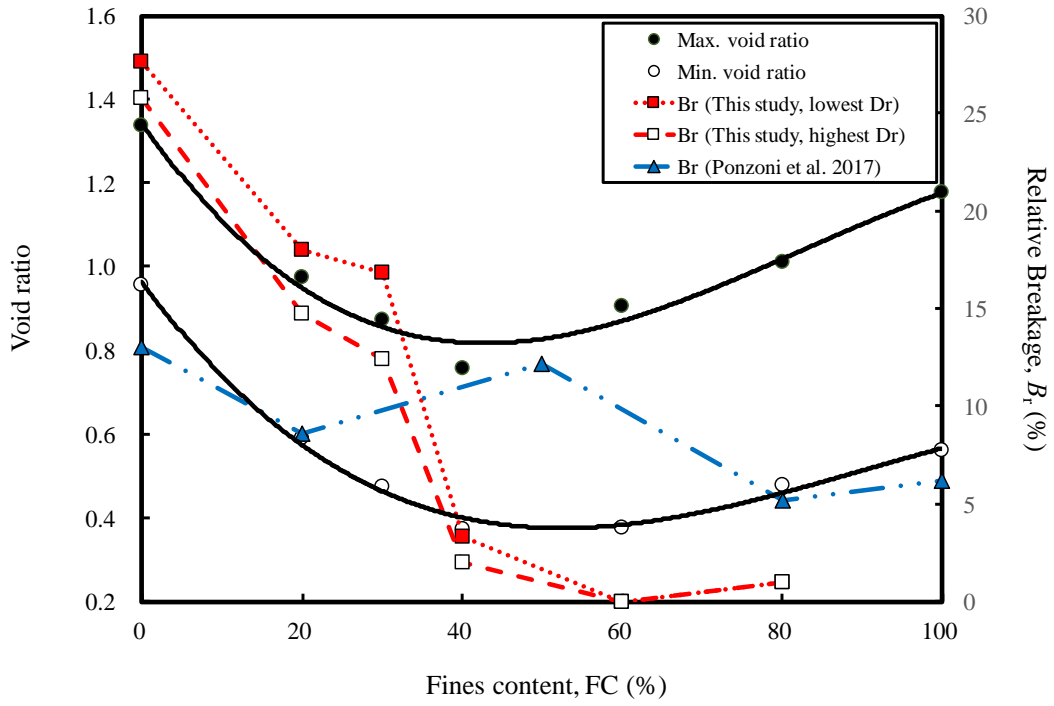
15

1
2



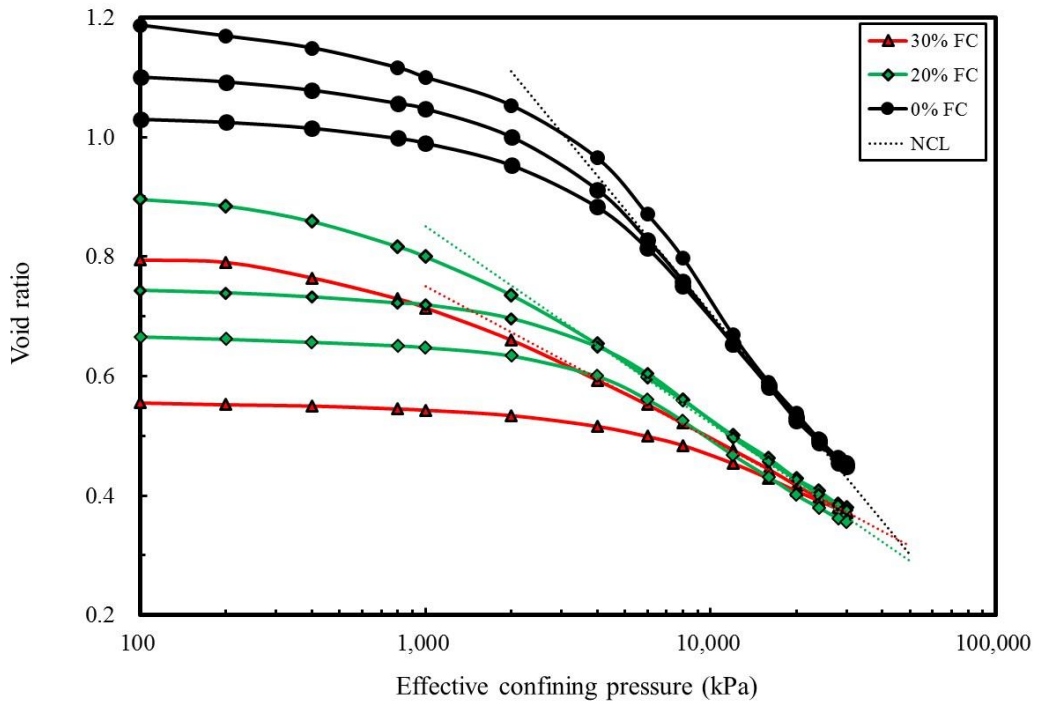
3
4
5
6
7
8
9
10
11
12
13
14
15
16
17
18
19
20
21
22
23
24
25
26
27

Fig. 1. Particle size distributions of CS-silt mixtures



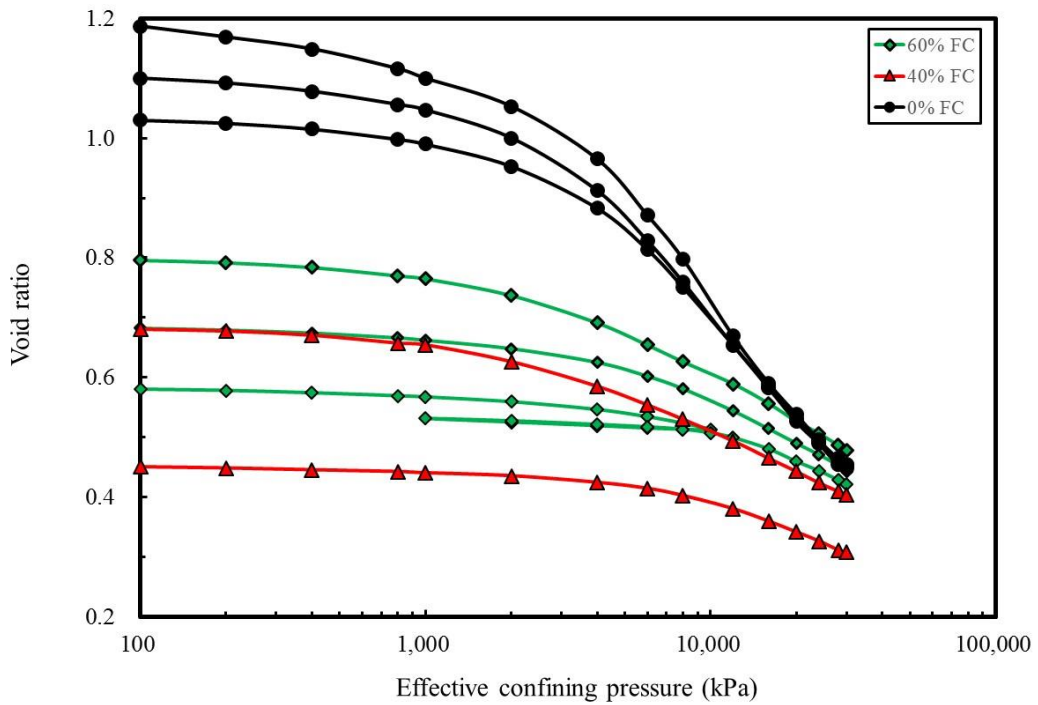
1
2
3
4
5
6
7
8
9
10
11
12
13
14
15
16
17
18
19
20
21
22
23
24
25
26
27

Fig. 2. Effects of fines content (FC) on (i) maximum and minimum void ratios, and (ii) relative breakage (B_r) of CS-silt mixtures



1
2

(a)

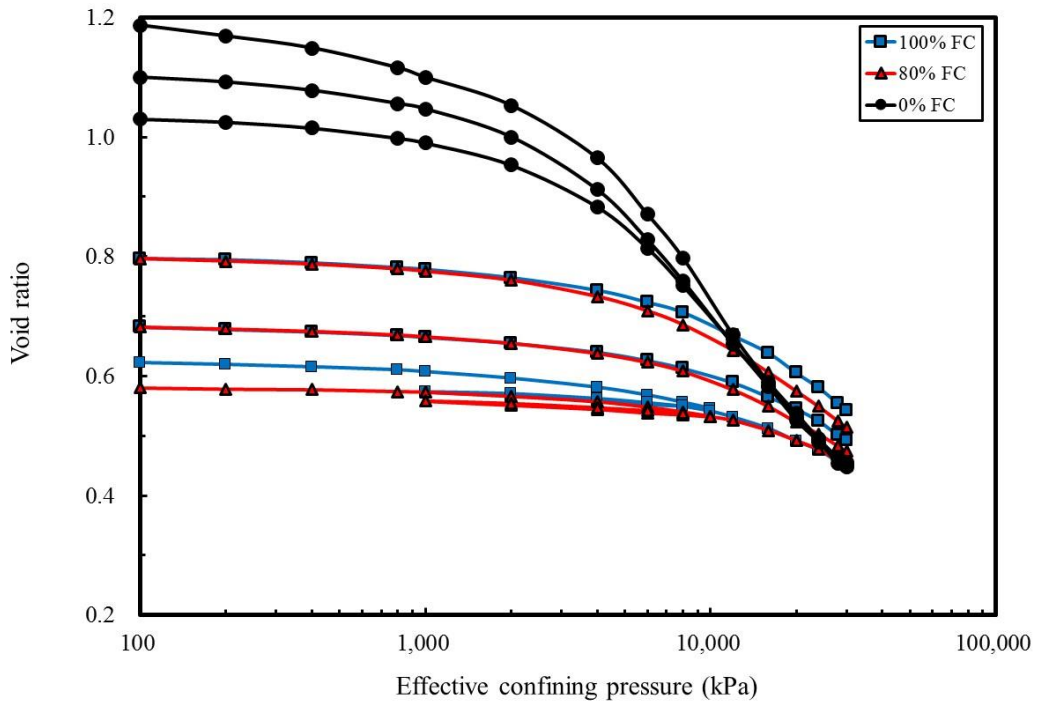


3
4
5

(b)

6 Fig. 3. Comparison of isotropic compression curves between CS–silt mixtures and pure CS (0%
7 FC): (a) 20 and 30% FC, (b) 40 and 60% FC, and (c) 80 and 100% FC

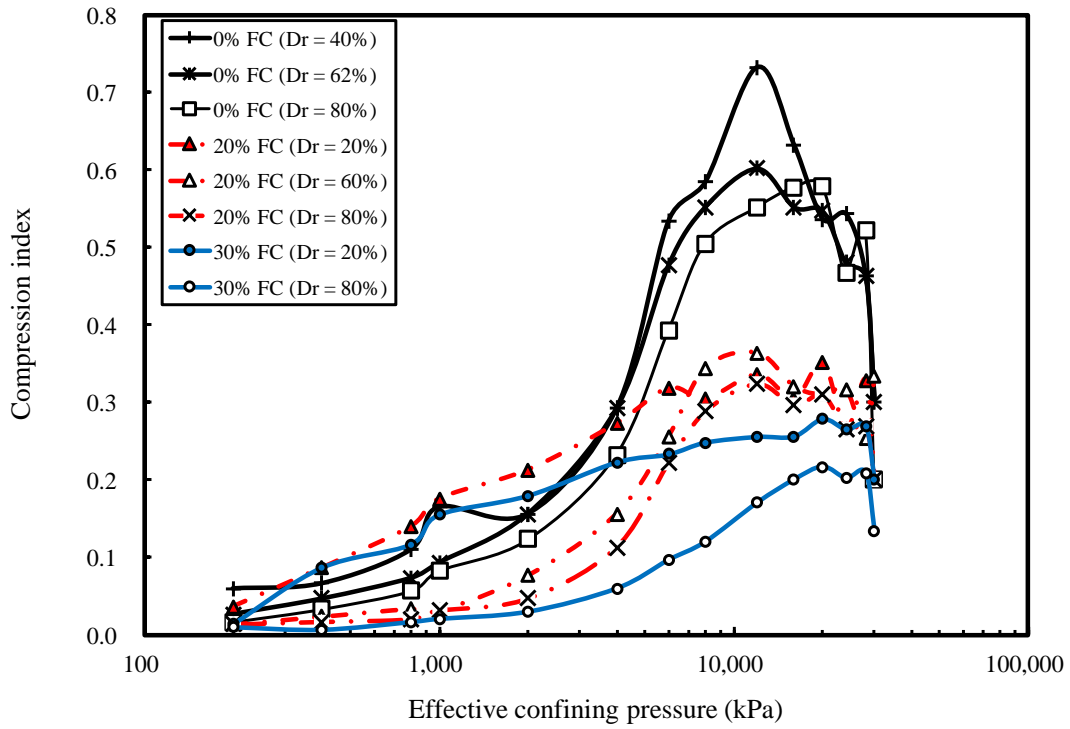
8
9
10
11
12



(c)

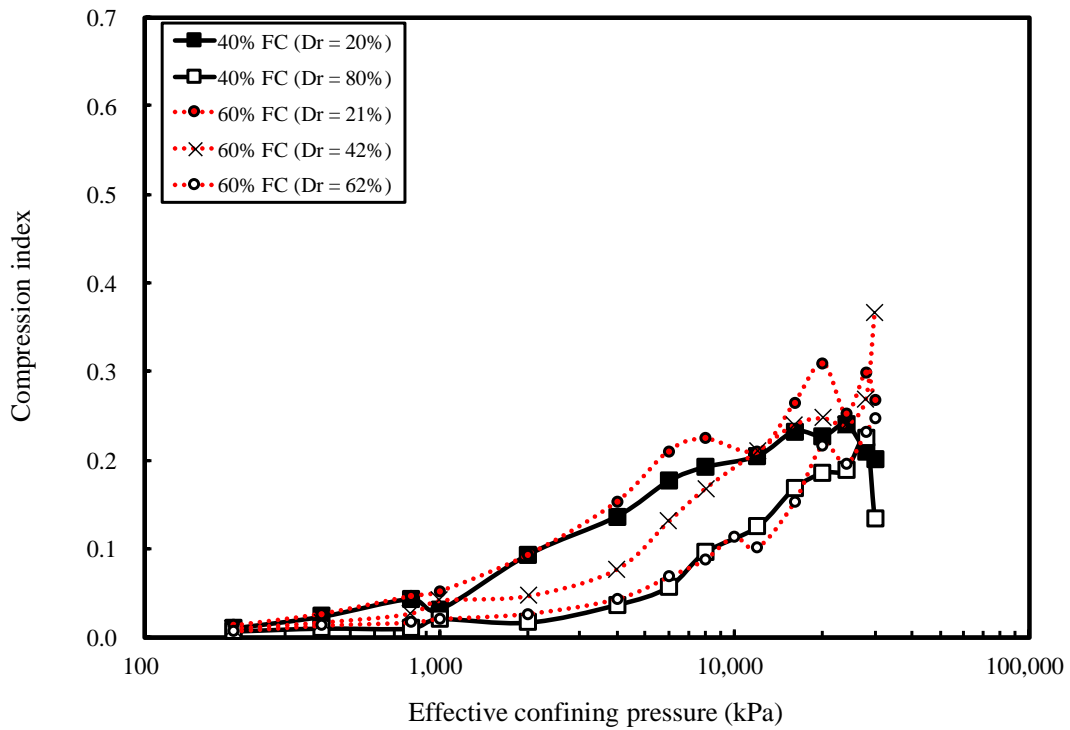
Fig. 3. Comparison of isotropic compression curves between CS-silt mixtures and pure CS (0% FC): (a) 20 and 30% FC, (b) 40 and 60% FC, and (c) 80 and 100% FC

- 1
- 2
- 3
- 4
- 5
- 6
- 7
- 8
- 9
- 10
- 11
- 12
- 13
- 14
- 15
- 16
- 17
- 18
- 19
- 20
- 21
- 22
- 23
- 24
- 25
- 26
- 27



1
2

(a)

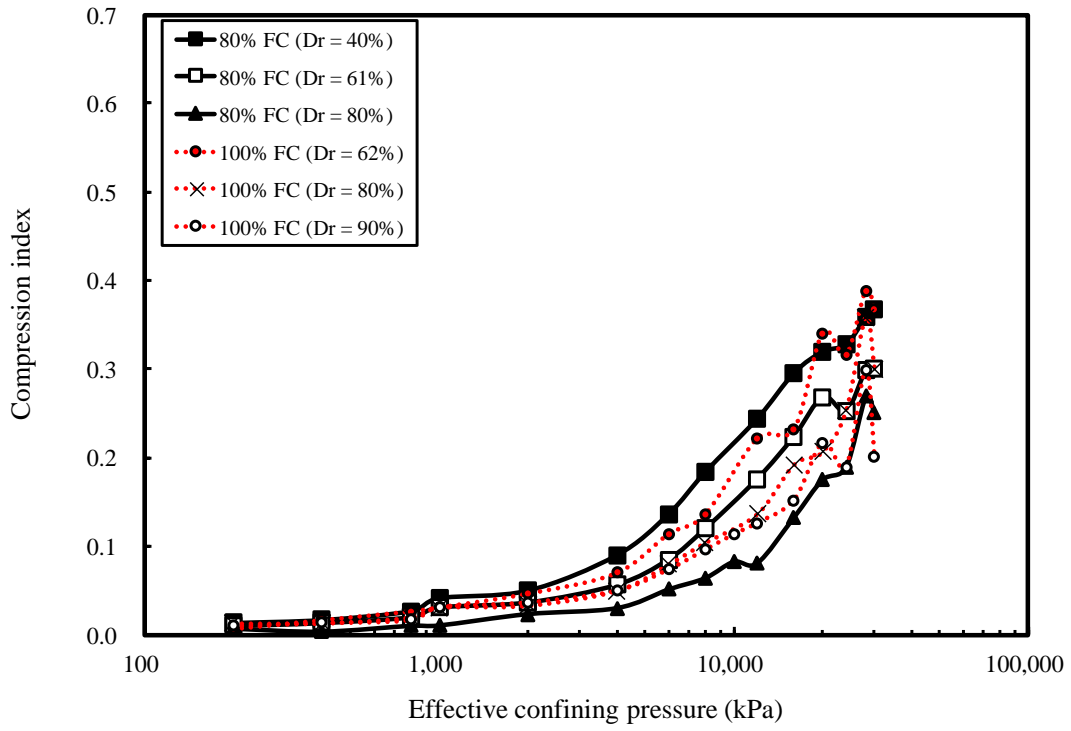


3
4

(b)

5 Fig. 4. Variation of compression index with effective confining pressure (a) 0–30% FC, (b) 40 and
6 60% FC, and (c) 80 and 100% FC

7
8
9
10



(c)

Fig. 4. Variation of compression index with effective confining pressure (a) 0–30% FC, (b) 40 and 60% FC, and (c) 80 and 100% FC

- 1
- 2
- 3
- 4
- 5
- 6
- 7
- 8
- 9
- 10
- 11
- 12
- 13
- 14